Proceedings of Symposium on Ultrasonic Electronics, Vol. 31 (2010) pp. 61-62
6-8 December, 2010

Measurement of Closed Fatigue Cracks with Nonlinear Ultrasonic Imaging Method Using Subtraction of Responses at Different Loads

荷重差分を用いた非線形超音波映像法による閉じた疲労き裂の測定

Makoto Hashimoto‡, Satoshi Horinouchi, Yohei Shintaku, Yoshikazu Ohara and Kazushi Yamanaka (Tohoku Univ.)
橋本 真琴‡, 堀之内 聡, 新宅 洋平, 小原 良和, 山中 一司 (東北大工)

1. Introduction

To measure closed crack depth, we have developed a novel imaging method, subharmonic phased array for crack evaluation (SPACE).[1)] SPACE provides fundamental array (FA) images at the frequency f and subharmonic array (SA) images at the frequency $f/2$, visualizing the open and closed parts of cracks, respectively. We have demonstrated its performance in closed fatigue and stress corrosion cracks.[1-4)] However, objects other than cracks such as coarse grains, weld defects and back surfaces, sometimes appear in subharmonic images owing to filter leakage, since short-burst input waves are used for obtaining high temporal resolution. The artifacts might degrade the performance of SPACE for identifying closed cracks.

In this study, to improve the selectivity of closed cracks from objects other than cracks, we propose a nonlinear ultrasonic imaging method 'load difference phased array' (LDPA) based on the subtraction of responses at different loads and phased array techniques, which is an extension of SPACE as well as another approach using a linear phased array (PA). Then, we show its performance for a closed fatigue crack on the basis of the static load dependence of SPACE images and the dynamic load dependence of PA images.

2. Principle of LDPA

A schematic illustration of the method is shown in **Fig. 1**. By applying external load to closed cracks, the contact state in the cracks varies, resulting in the intensity change of responses at cracks.[5)] In contrast, the responses at objects other than cracks are independent of external load. Therefore, the subtraction of the responses at loads L_1 and L_2 enables us to extract only the cracks.

The above idea is formulated for the quantitative evaluation of the method. The image intensity at position $\mathbf{r}$ under an applied load L is given by

$$I^{L}{}_{P,F,S}(\mathbf{r}) = \sqrt{\int_{t_C}^{t_C+\tau} \left| u^{L}{}_{P,F,S}(\mathbf{r},t) \right|^2 dt}, \qquad (1)$$

where t_C is the correction factor for propagation in the wedge and electronic trigger delay, and

$$u^{L}{}_{P,F,S}(\mathbf{r},t) = \sum_{n=1}^{N} u^{L}{}_{P,F,S,n}(t - t_n(\mathbf{r})) \qquad (2)$$

where n is the number of elements, N is the total number of elements, $t_n(\mathbf{r}) = (|\mathbf{r}_s - \mathbf{r}| + |\mathbf{r} - \mathbf{r}_n|)/V$ is the propagation time from the source at position $\mathbf{r}_s$ to the nth element at position $\mathbf{r}_n$ via the image position $\mathbf{r}$. For a particular crack of known length and depth, the subtracted images are given by

$$\Delta I_{P,F,S}(K_1, K_2, \mathbf{r}) = I^{K_1}{}_{P,F,S}(\mathbf{r}) - I^{K_2}{}_{P,F,S}(\mathbf{r}) \qquad (3)$$

where K_1 and K_2 are the stress intensity factors for the crack at loads L_1 and L_2, respectively.

For the application of external load to cracks, static or dynamic loading can be employed. For static loading, the method utilizing a hydraulic pump and a jig, e.g., the four-point bending test, is effective. For dynamic loading, a low-frequency vibrator is used. In this study, as a preliminary experiment, we simulated static and dynamic loads with a servohydraulic fatigue testing machine, which has been used for forming closed fatigue crack.

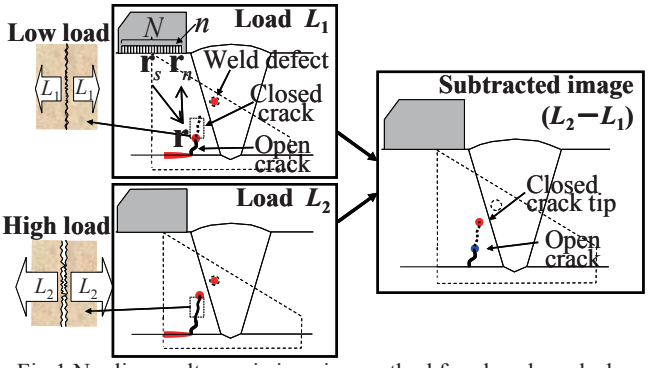

Fig.1 Nonlinear ultrasonic imaging method for closed cracks by subtraction of responses at different loads.

3. Specimen[4)]

We used a compact tension (CT) specimen having a closed fatigue crack with 10 mm deep made of aluminum alloy (A7075) with a maximum stress intensity factor of 9.0 MPa·m$^{1/2}$ and a minimum stress intensity factor of 0.6 MPa·m$^{1/2}$.[4)]

4. Experimental results

4.1 Static load dependence of SPACE images[6)]

To demonstrate the proposed method, we imaged a closed crack using SPACE while applying static load of K_1 = 0.5 and K_2 =1.3 MPa·m$^{1/2}$. Then, the subtraction of FA and SA images was carried out between K_1 and K_2. As a result, $\Delta I_S(K_2, K_1)$ shows a decrease in the intensity of response at crack tip. At $\Delta I_F(K_2, K_1)$, the artifacts were

eliminated; therefore we succeeded in extracting only the increase in the intensity of response at crack.

4.2 Dynamic load dependence of PA images

We recorded the dynamic change in a closed crack in PA images in real time, under sinusoidal loading with K =0 MPa·m$^{1/2}$ to 7 MPa·m$^{1/2}$ at a frequency of 0.1 Hz. A schematic of the experimental configuration is shown in **Fig. 2**. Here, we used an array sensor having 32 elements with a center frequency of 5 MHz for PA.

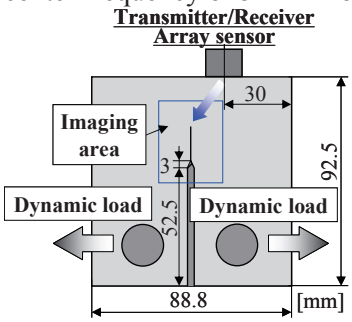

Fig. 2 Schematic of experimental configuration for PA and dynamic loading.

Snapshots of the dynamic load dependence of PA image are shown in **Figs. 3(a)-(h)**. The crack cannot be observed in **Figs. 3(a)-(d)**, whereas it is visible in **Figs. 3(e)-(h)**. This shows that the closed-crack tip was opened by the loading. We then precisely examined the intensity change of responses at the crack tip at 0.25 s intervals (**Fig. 4**). Above K =2.4 MPa·m$^{1/2}$, the intensity was saturated. This suggests that the crack was completely open in this region. Accordingly, the closure stress was estimated to be approximately K =2.4 MPa·m$^{1/2}$. By subtraction of **Figs. 3(h)** and **(a)**, the corner on the left side of the notch, which is strong linear scatterer, was eliminated in $\Delta I_P(K_3, 0)$ of **Fig. 5**, where K_3 =7.0 MPa·m$^{1/2}$, although the tip and the corner on the right side of the notch were visualized because they were affected by the crack opening/closing behavior. Consequently, we succeeded in imaging the increase in the intensity of response at the crack tip and the decrease in such intensity at the root of the crack. We demonstrated that the subtraction method can extract the parts related to a closed crack.

5. Discussion

As an indication of the selectivity, the intensity ratio of cracks to objects other than cracks such as linear scatterers or artifacts is defined as

$$S = I_c / I_l , \qquad (4)$$

where I_c is the intensity at the crack and I_l is that at linear scatterers or artifacts. **Fig. 6** shows S in the SPACE and PA images before and after the subtraction. As a result of the subtraction, S in the FA and SA images were improved by factors of 3.6 and 3.3 by canceling the artifacts. For the PA images, S was markedly improved by a factor of 24 by canceling the strong linear scatterer. Thus, we demonstrated that the method of LDPA is very useful in improving the selectivity of closed cracks from linear scatterers or artifacts.

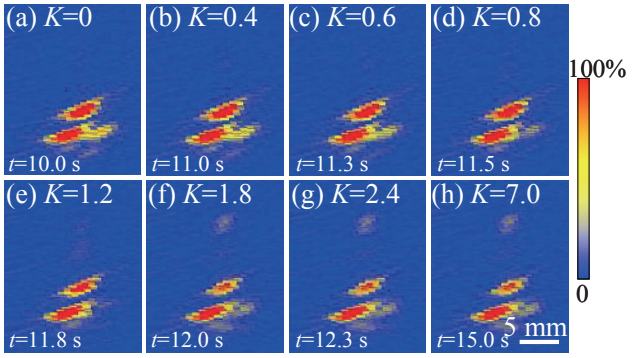

Fig. 3 Snapshots of dynamic load dependence of PA image; (a) PA images at K=0, (b) K=0.4, (c) K=0.6, (d) K=0.8, (e) K=1.2, (f) K=1.8, (g) K=2.4, (h) K=7.0 MPa·m$^{1/2}$.

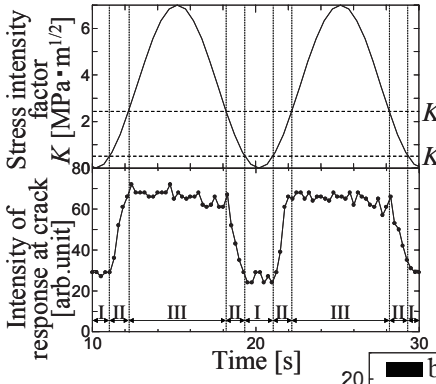

Fig. 4 Dynamic load measured by a load cell attached servohydraulic fatigue testing machine and the intensity of response at the crack tip.

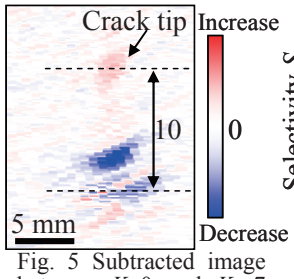

Fig. 5 Subtracted image between K=0 and K_3=7 MPa·m$^{1/2}$.

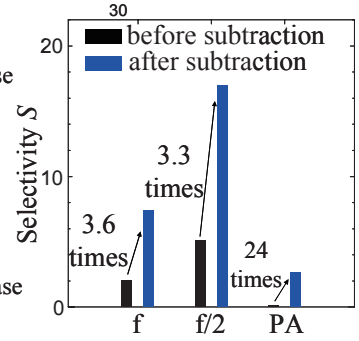

Fig. 6 Selectivity of closed cracks from scatterers or artifacts.

6. Conclusions

In this study, we proposed a nonlinear ultrasonic imaging method, load difference phased array (LDPA), and performed experiments on a closed fatigue crack. As a result, only the intensity change of responses at closed cracks was extracted with high selectivity. Thus, we demonstrated that LDPA is very useful in improving the selectivity of closed cracks from objects other than cracks.

Acknowledgment; This work was supported by Grant-in Aid for Scientific Research.

References: 1) Y. Ohara, T. Mihara, R. Sasaki, T. Ogata, S. Yamamoto, Y. Kishimoto, K. Yamanaka: Appl. Phys. Lett. **90** (2007) 011902. 2) Y. Ohara, S. Yamamoto, T. Mihara, K. Yamanak:, Jpn. J. Appl. Phys. **47** (2008) 3908. 3) Y. Ohara, H. Endo, T. Mihara, K. Yamanaka: Jpn. J. Appl. Phys. **48** (2009) 07GD01. 4) Y. Ohara, H. Endo, M. Hashimoto, Y. Shintaku, K. Yamanaka: Rev. Prog. QNDE **29** (2010) 903. 5) V. V. Kazakov, A. Sutin, P. A. Johnson: Appl. Phys. Lett. **81** (2002) 646. 6) M. Hashimoto, Y. Ohara, H. Endo, Y. Shintaku, K. Yamanaka: Proc. 30th Symp. Ultrasonic Electronics, 2009, p. 69.